**Advances in Computational Design**, *Vol. 10, No. 1 (2025) 35-50*
https://doi.org/10.12989/acd.2025.10.1.035


# Artificial neural network modelling for predicting tribological properties of Al8090/$TiB_2$/C composites using optimized hyperparameters

Mohamed Zakaulla*

*Department of Mechanical Engineering, H.K.B.K College of Engineering, Bangalore 560045, India*
*Visvesvaraya Technological University, Belagavi, Karnataka, India*

*(Received September 26, 2024, Revised December 23, 2024, Accepted December 26, 2024)*

**Abstract.** This study introduces a new framework that utilizes artificial neural networks (ANN) to analyze data and forecast the tribological properties of Al8090/$TiB_2$/C composites. For training a multi-layered artificial neural network (ANN), a total of 1920 input datasets are used. These datasets are created by combining six input parameters, including the volume of Al8090 matrix, Titanium diboride, and Graphene, as well as the load, sliding speed, and sliding distance. The corresponding output consists of specific wear rate and coefficient of friction. A surrogate model for predicting the tribological properties has been developed by optimizing the hyperparameters to enhance the accuracy of the model's predictions. The results of the ANN-based approach validate that the proposed model has a mean absolute percentage error of 3.42% for the predictions of specific wear rate in dry sliding wear test scenarios, and a MAPE of 0.28% for the predictions of coefficient of friction.

**Keywords:** aluminium; artificial neural network; hyperparameters; graphene; tribology

## 1. Introduction

The performance and dependability of materials face significant challenges in applications that need wear resistance due to increased tribological effects and reduced lubrication efficiency. The tribological characteristics, encompassing friction, wear, and lubrication, are crucial elements in evaluating the suitability of materials for demanding environments. The desire to achieve enhanced tribological performance has motivated extensive research and development efforts in the pursuit of new materials. The favourable attributes of aluminum alloys, including their elevated strength, exceptional resistance to corrosion, and lightweight nature, have resulted in their substantial consideration for use in high-wear applications. Al8090 alloys are utilized in marine, aerospace, and electronic components due to their low weight, excellent malleability, and ability to resist corrosion (Singh *et al*. 2004, Lynch *et al*. 2001). The wear resistance of Al8090 alloys can be significantly enhanced by carefully choosing various reinforcing materials or fillers, such as titanium diboride and graphene, to improve their tribological performance. Titanium diboride is

*Corresponding author, Professor, E-mail: zakaulla.me@hkbk.edu.in


http://www.techno-press.org/?journal=acd&subpage=7 ISSN: 2383-8477 (Print), 2466-0523 (Online)

utilized in specific fields such as impact-resistant armor and wear-resistant coatings (Akin and Kaya 2017, Kumar *et al*. 2024, Zhou *et al*. 2023). Graphene possesses inherent characteristics of low-friction, high stiffness, and the potential to decrease friction and wear through its thermal conductivity.

Ref. (Kazi *et al*. 2020) developed the artificial neural network models to accurately forecast the load-displacement curves of cotton fiber/polyvinyl chloride (PVC) composites. The ANN models were trained and evaluated based on the experimental data using the back-propagation approach, and prediction was achieved using grid search hyperparameter. The implemented methodology demonstrated high efficacy, significantly minimizing the time and effort required for behavioral studies involving multiple samples. This will greatly assist materials designers in properly planning their future research. Ref. (Cheung *et al*. 2024) performed micro-mechanical modeling of non-linear path-dependent materials requiring a significant amount of computational resources. A new method was presented for data augmentation, which allows for the expansion of an existing dataset without the need for extra computational simulations. An RNN was trained and verified using simulations of elasto-plastic short fiber reinforced composites. The results demonstrated a significant enhancement in the network's predictions when trained on enlarged datasets utilizing the suggested data augmentation technique. The suggested approach for enhancing limited data can be used not only to other types of composites, but also to various materials and at different scales. Ref. (Manu *et al*. 2024) studied carbon fiber reinforced polymers (CFRP) which were enhanced by including polycarbonate (PC)/acrylic butadiene styrene (ABS) and depositing silanized graphene oxide onto the carbon fibers via electrophoretic deposition. The Levenberg-Marquardt algorithm, artificial neural network, and linear regression were employed to forecast wear behavior. The Matlab-based Neural Network technique achieved the lowest mean squared error (MSE) loss, with 0.35% MSE for RT samples and 0.88% for CT samples. This study aims to improve the understanding and performance of CFRP materials in wear-resistant applications through the utilization of optimization methodologies. Ref. (Provencher *et al*. 2024) reported on the effects of patch size, training data volume, and data augmentation on deep learning performance on a constrained set of data. They examined U-Net model training using four distinct fiber-reinforced composite samples. seven-fold replication of every experimental condition was used as the training process is non-deterministic, which helped to prevent under sampling and track the variance in the model's training. It was found that higher volumes of training data improve the final accuracy and learning speed of individual models while lowering the variance between replicates. scientific imaging semantic segmentation models employ large coefficients of data augmentation. Ref. (Jung and Chang 2021) presented a system for monitoring the structural health of intelligent composite structures by employing signal processing and deep learning algorithms. Piezoelectric ribbon sensors were used into composite laminates for the purpose of enabling self-monitoring. The impact signals were subjected to a discrete wavelet transform in order to turn them into input image data for the convolutional neural network models. Data augmentation was also utilized to ensure an adequate amount of data for training the impact characterisation model. Finally, the performance of neural network models was evaluated by comparing the test errors for each condition applied. Ref. (Azad and Kim 2024) reported a strong and independent method for diagnosing damage in laminated composite constructions. The method utilizes hybrid deep convolutional networks to accurately identify and assess the extent of the damage. The hybrid models integrate the benefits of both convolutional procedures for extracting profound features and SVM for diagnosing with limited feature data. The validity of the proposed hybrid models is confirmed by testing them with randomly generated vibrational signals

representing a healthy condition and two states of delamination in laminated composites. The results demonstrated enhanced efficacy in detecting damage compared to traditional approaches, while also requiring less computational resources. This paper employs an Artificial Neural Network model to predict the tribological characteristics of Al8090 composites. The correctness of the model is evaluated by analyzing input design parameters, while the specific wear rate and coefficient of friction are obtained by a dry sliding wear test. Further in this study, it provides a comprehensive account of the stir casting process, the conduction of wear tests specifically for Al8090 composites, and the creation of a database that serves as input for training the ANN model. It outlines the ANN architecture, the process of training and testing the proposed model, and the adjustment of hyperparameters to get an optimized ANN model for Al8090 composites. The accuracy of the optimized Artificial Neural Network (ANN) model's predictions is confirmed through wear test results.

## 2. Methodology

The study's technique, which aims to simplify the tribological charateristics of the Al8090/$TiB_2$/C composites prediction model, is shown in Fig.1. For every dataset, ANN is trained to predict the tribological properties of Al8090 composite. The following lists the steps that make up this framework.

• A description of the wear test and material composition crucial parameters used as input parameters. The Al8090 matrix volume, Titanium diboride volume, Graphene volume, load, sliding speed, and sliding distance are the chosen input parameters. The input dataset is prepared and processed using Min-Max Normalization approach to define the maximum and minimum limits of the input parameters. The output comprises the tribological properties such as specific wear rate and coefficient of friction that are determined by wear tests.

• Artificial neural network models are trained and tested using different activation functions, epochs, batch sizes, and learning rates. The ANN model is optimised by adjusting the hyperparameters to enhance the prediction of specific wear rate and coefficient of friction. The output from the wear test results is compared with the projected tribological properties, and the optimal ANN model is finally provided.

• The test dataset assesses the correctness of the ANN model's performance. Multiple artificial neural network (ANN) models are created by utilizing the training dataset with varying hyperparameters. Next, the trained artificial neural network models are used to predict the tribological features of each set in the training dataset. Various models are trained using the metrics of mean absolute error (MAE) and mean squared error (MSE). The final artificial neural network (ANN) model is selected based on the optimised model that has the lowest mean absolute percentage error (MAPE).

### *2.1 Fabrication and dry sliding wear test of Al8090/TiB2/C composites*

The Al8090/$TiB_2$/C composites are produced by a liquid metallurgical process employing a stir casting technique. The preheated $TiB_2$ powder and graphene, with varying proportions, were introduced in to the Aluminum alloy. The Al8090 composite underwent mechanical stirring with reinforcement for a duration of 10 minutes at a rotational speed of 250 revolutions per minute. The molten composite was poured into the preheated cast-iron molds while keeping the temperature at

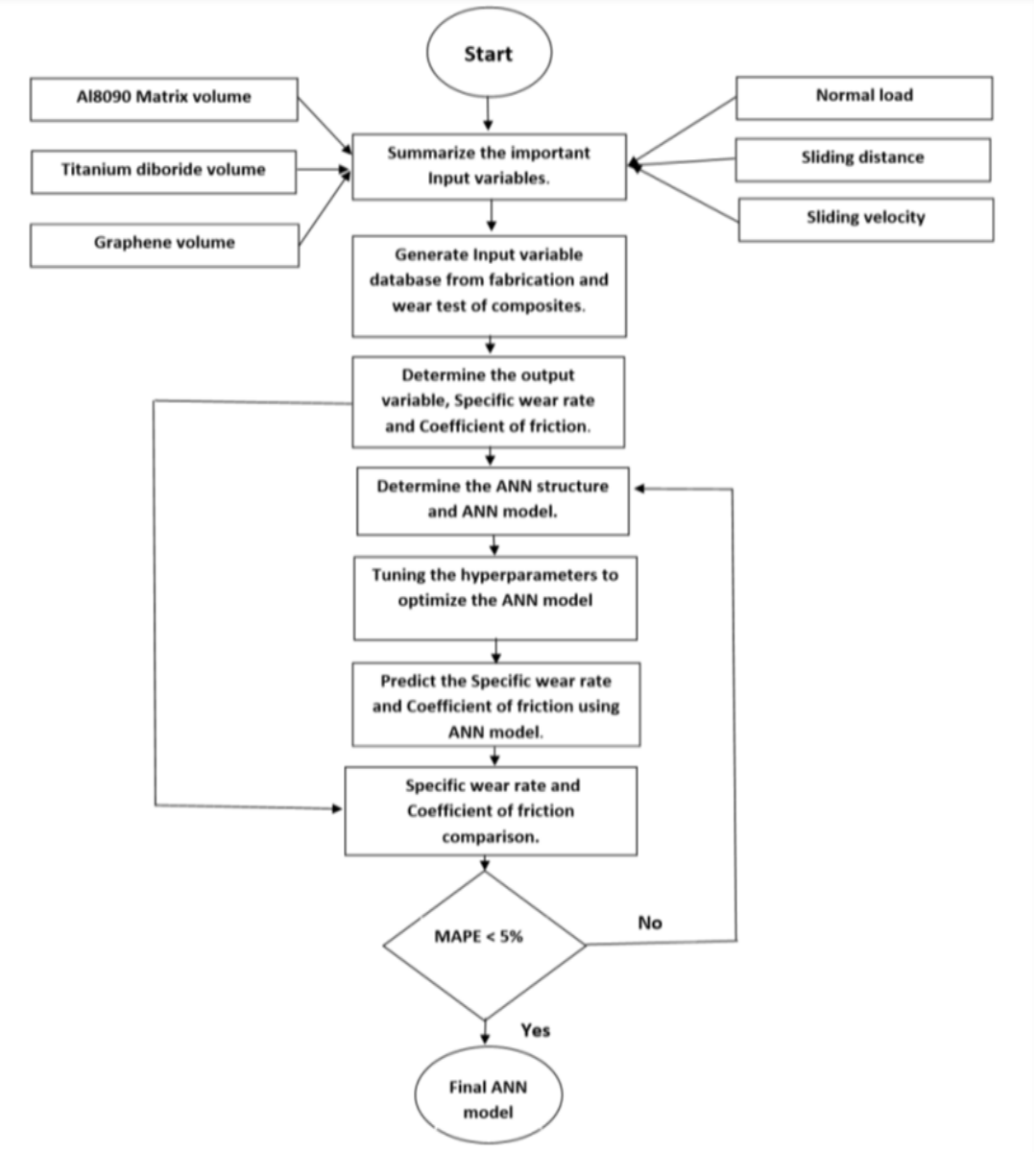


Fig. 1 Methodology flow chart

800° C. The $TiB_2$ concentration in the matrix alloy was varied at 2 -10 weight percent. In addition, the alloy consisted of different proportions of graphene: 0.5-2 weight percent.

Fig. 2 shows a dry sliding wear test was performed according to ASTM G99 standard on a steel disk with a hardness of Rc60. Specimens made of Al8090/$TiB_2$/C composites with varied percentage of reinforcements such as titanium diboride (2-10wt%) and graphene (0- 2wt%) are tested at a load of 10N, 20N, 30N, and 40N, respectively. Fig. 3 shows specimens having a diameter of 9mm and a length of 30mm are tested at room temperature at a speeds of 0.5m/s, 1m/s,


Fig. 2 Tribometer testing setup for wear analysis

Fig. 3 Specimens of Al8090/$TiB_2$/C composite used for wear test

1.5m/s, and 2m/s. The specimens were grinded and polished for smooth finish and later cleaned with ethanol and dried before the wear test. The sliding distance is essential for determining the specific wear rate, as it directly influences the volume of material lost to wear. During the testing, real-time data on frictional forces were documented utilizing sensors embedded in the tribometer. The coefficient of friction was calculated by averaging the friction force data obtained during the test and dividing it by the applied load. The specific wear rate is calculated using the equation.

$$\text{Specific wear rate} = \frac{\text{volume}}{\text{load x sliding distance}} \quad (1)$$

## 3. Machine learning modelling

### *3.1 Artificial neural network*

The database comprises input variables and corresponding output data, creating a complete database for artificial neural network (ANN) modelling. The database is partitioned into two distinct sets, namely the training set and the test set, in order to construct an Artificial Neural Network model. The database is partitioned into 70% (1344) for training and 30% (576) for testing

Table 1 Input parameter minimum and maximum values

| Input parameter | Minimum value | Maximum value |
|---|---|---|
| AI8090 matrix volume [wt%] | 88 | 97.5 |
| Titanium diboride volume [wt%] | 2 | 10 |
| Graphene volume [wt%] | 0.5 | 2 |
| Load (N) | 10 | 40 |
| Sliding speed (m/s) | 0.5 | 2 |

Table 2 Components used in architecture of neural network

| Network | Number |
|---|---|
| Input layer | 6 |
| Hidden layer | 2 |
| Output layer | 2 |

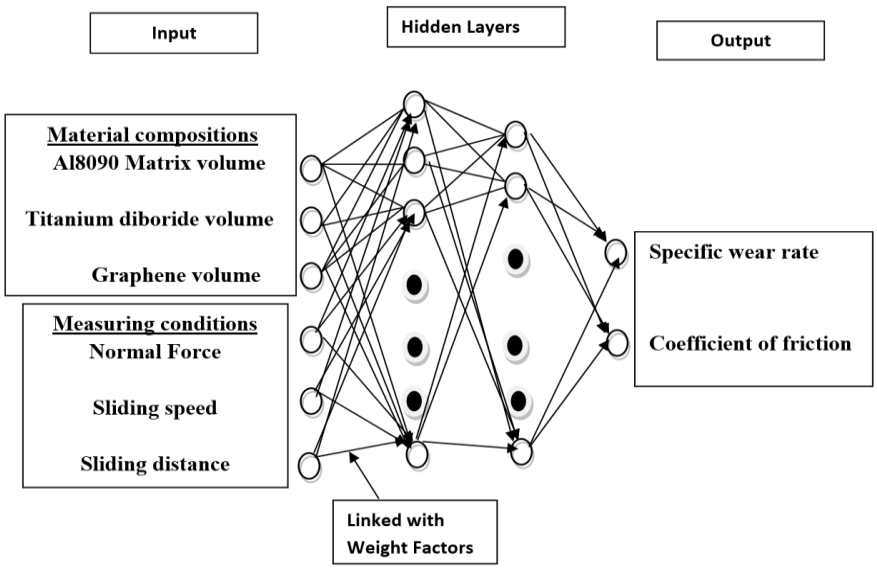


Fig. 4 Diagram of artificial neural network for material composition and measuring conditions

the Artificial Neural Network model. The training dataset is utilized to determine the weights and bias parameters in order to build an Artificial Neural Network model that can accurately predict tribological features. Hyperparameters are optimized by employing a subset of the training dataset in order to minimize prediction error (Provencher *et al*. 2024, Lujan-Moreno *et al*. 2018, Afape *et al*. 2024, Lima *et al*. 2023, Wang *et al*. 2022).

The database is composed of different combination of input parameters, as shown in Table 1. The training process has a major impact on the model's prediction accuracy. In this work, the multi-layer perceptron artificial neural network is used. The components used in architecture of neural network is shown in Table 2, whereas the architecture of the ANN used in this study is shown in Fig. 4. The suggested artificial neural network design comprises one layer for input, two

Table 3 Comparison of different ANN models

| Activation function for Hidden layers 1 and 2 | Nodes Layer 1 | Nodes Layer 2 | Cost | Specific wear rate Train dataset | Specific wear rate Test dataset | Coefficient of friction Train dataset | Coefficient of friction Test dataset |
|---|---|---|---|---|---|---|---|
| Leaky ReLU | 200 | 100 | MAE | 0.49 | 0.74 | 0.001 | 0.001 |
| | | | MSE | 0.53 | 1.17 | 3.69 | 1.83 |
| ELU | | | MAE | 0.48 | 0.75 | 0.001 | 0.001 |
| | | | MSE | 0.60 | 1.28 | 7.19 | 6.84 |
| SeLU | | | MAE | 0.49 | 0.70 | 0.001 | 0.001 |
| | | | MSE | 0.63 | 0.99 | 3.45 | 3.44 |
| ReLU | | | MAE | 0.32 | 0.64 | 0.0001 | 0.0001 |
| | | | MSE | 0.38 | 0.94 | 3.24 | 1.03 |

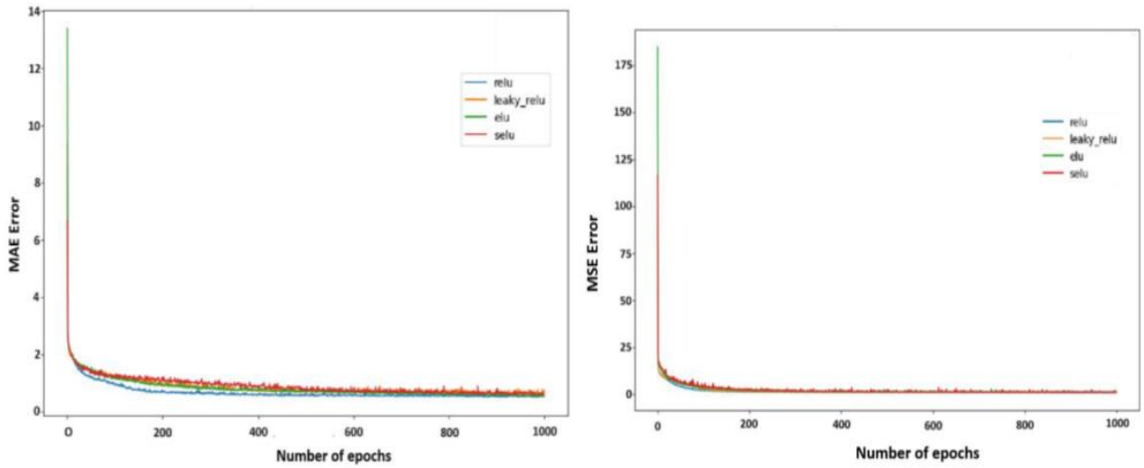


Fig. 5 Variation of (a) MAE and (b) MSE with epochs for different activation functions for specific wear rate

hidden layers and one output layer. Multiple combinations of hyperparameters are analyzed to determine the most precise and suitable artificial neural network model for the existing database. The proposed model with the lowest Mean MAPE for the Test dataset is chosen as the final Artificial Neural Network model. The hidden layer in this study is made up of two layers. Several activation functions are commonly employed in artificial neural networks as discussed in previous studies (Hasan *et al*. 2024, Babaei *et al*. 2022).

Table 3 displays the activation functions used in the current investigation and MAE and MSE are both types of loss functions. The Adam optimizer is employed to identify the optimal hyperparameters that result in precise predictions from the network. The loss is minimized by utilizing an optimizer to adjust the settings, which have been enhanced to achieve the lowest possible loss. The comprehension and acquisition of ANN architecture include utilizing the PyTorch package in Python. In this study, four activation functions are examined, which are listed in Table 3. Eight artificial neural network models have been created by merging activation functions with two loss functions. MAE and MSE serve as loss functions for determining the

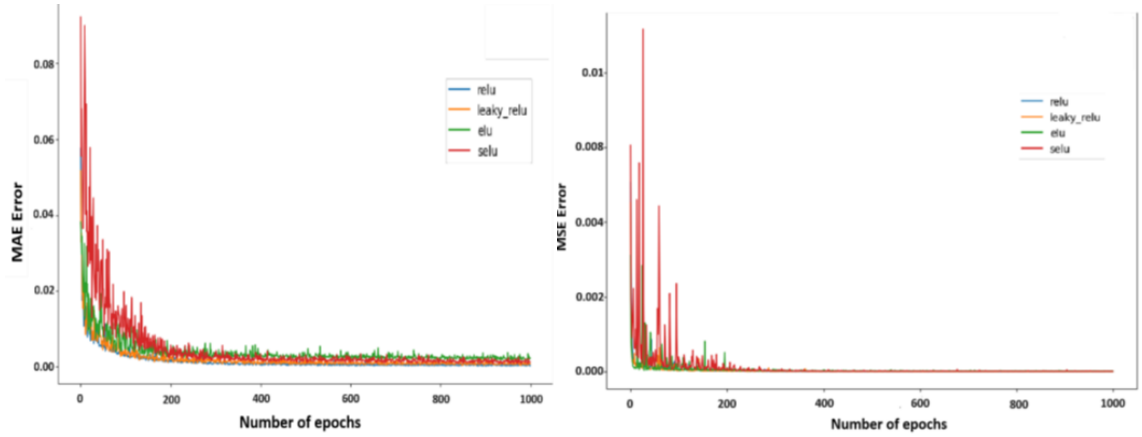


Fig. 6 Variation of (a) MAE and (b) MSE with epochs for different activation functions for coefficient of friction

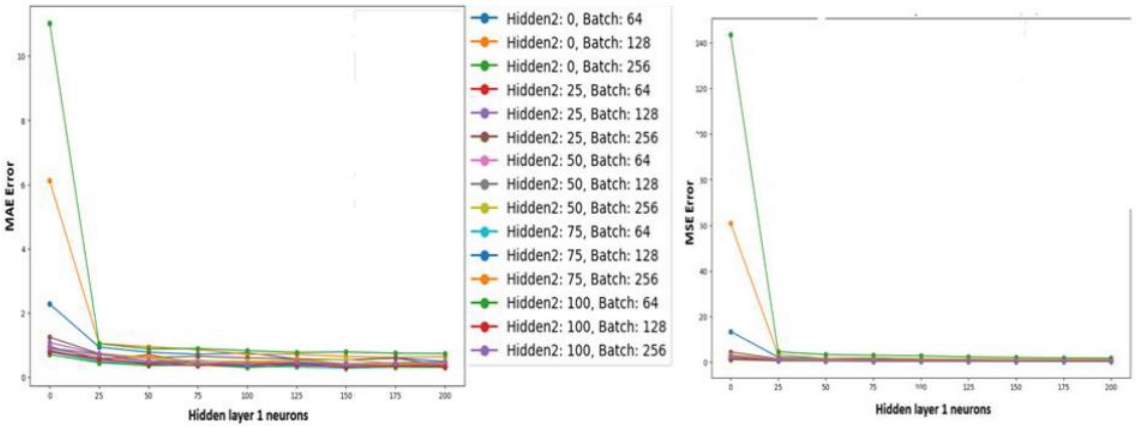


Fig. 7 Variation of (a) MAE and (b) MSE for a distinct combinations of batch sizes and the number of neurons in hidden layers for specific wear rate.

variation between the actual tribological characteristics obtained through dry sliding wear tests and the predicted tribological parameters such as specific wear rate and coefficient of friction. The activation function is chosen initially while leaving the other parameters constant. The Mean Absolute Error and Mean Squared Error are the loss functions for each activation function at 1000 epochs, as shown in Table 3. In order to choose the most appropriate activation function for the present database, epoch, nodes in hidden layers, batch size, and learning rate are been kept constant. Table 3 displays the Artificial Neural Network (ANN) models, each utilizing distinct activation functions. The first hidden layer consists of 200 neurons, while the second hidden layer comprises 100 neurons. Table 3 indicates that the ReLU and eLU activation functions have significantly lower MAE and MSE values. However, ReLU has a partly lesser error than eLU. This is validated by the predicted error for the test datasets, as depicted in Fig. 5 and Fig. 6. It demonstrates that the ReLU activation function yielded the least error for both the MSE and MAE loss functions for both specific wear rate and coefficient of friction. Test error, ReLU is henceforth regarded as an optimized activation function based on this.

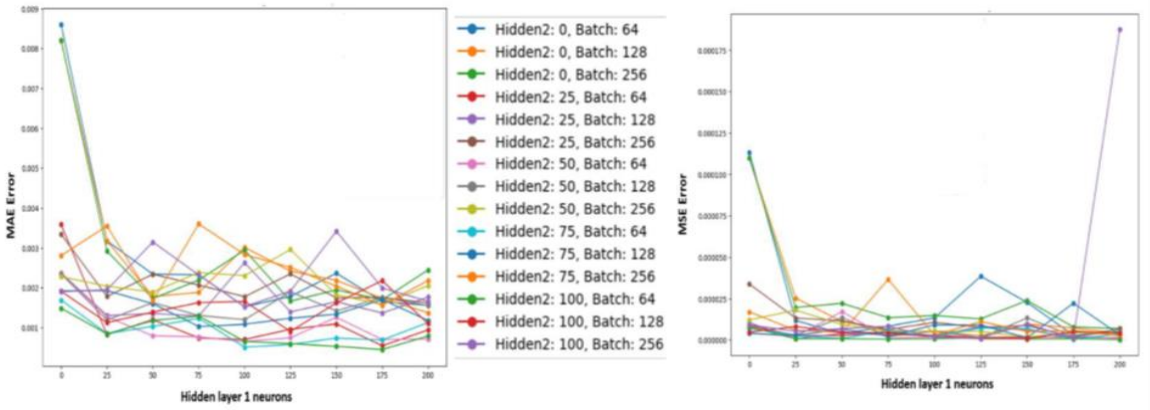


Fig. 8 Variation of (a) MAE and (b) MSE for a distinct combinations of batch sizes and the number of neurons in hidden layers for coefficient of friction

Table 4 A comparison of the efficiency of Relu for various hidden layer neurons with a batch size of 64 for a specific wear rate

| Activation function in hidden layers (1 and 2) | Nodes L1 | Nodes L2 | Cost | Train | Test |
|---|---|---|---|---|---|
| ReLU | 150 | 100 | MAE | 0.32 | 0.33 |
| | 150 | 100 | MSE | 0.32 | 0.34 |
| | 175 | 100 | MAE | 0.29 | 0.30 |
| | 175 | 100 | MSE | 0.3 | 0.32 |

Table 5 A comparison of the efficiency of Relu for various hidden layer neurons with a batch size of 64 for coefficient of friction

| Activation function in hidden layers (1 and 2) | Nodes L1 | Nodes L2 | Cost | Train | Test |
|---|---|---|---|---|---|
| ReLU | 200 | 100 | MAE | 0.005 | 0.009 |
| | 200 | 100 | MSE | 0.001 | 0.004 |
| | 175 | 100 | MAE | 0.0004 | 0.0008 |

### *3.2 Optimization of the quantity of hidden neurons and batch size:*

The optimal hidden layer neurons is determined by various parameters, including the training technique, difficulty of the problem and size of the database. Generally, increasing the number of neurons or layers in a deep network can lead to overfitting problems and result in lesser prediction accuracy. Conversely, a network constructed with an inadequate number of neurons and layers is unable to comprehend the intricate connection between the input and output, resulting in a significant margin of error in predictions. Therefore, it is imperative to optimize the quantity of neurons in order to improve the accuracy of the model's predictions (Wang *et al*. 2024).

The neurons in hidden layer 1 ranges from 25 to 200, with an interval of 25 neurons. In hidden layer 2, the neurons ranges from 25 to 100, with an interval of 25. The batch size has been set to 64, 128, and 256, which is commonly employed in machine learning. The Mean Squared Error and

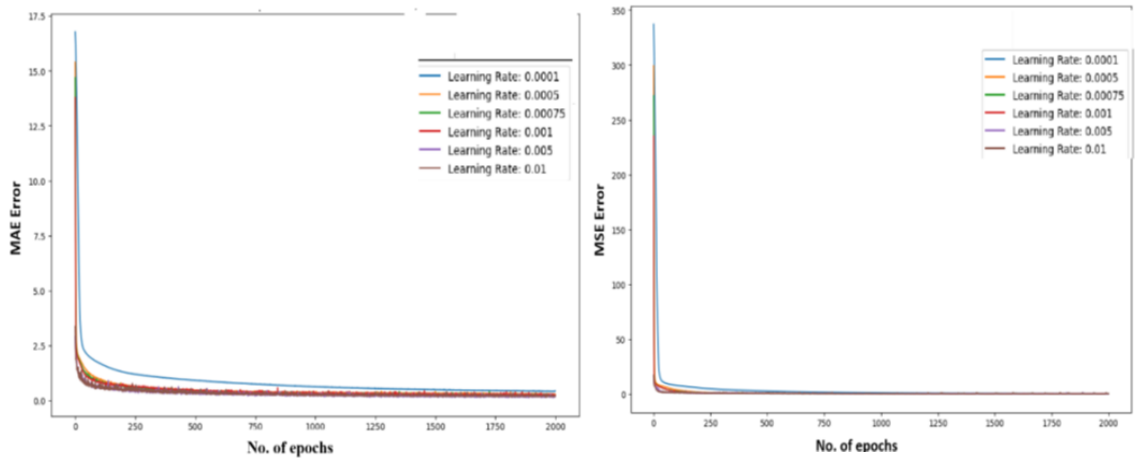


Fig. 9 Variation of a) MAE b) MSE for test data set for different learning rates and epochs for specific wear rate

Mean Absolute Error decreases and stabilize as the quantity of neurons in the hidden layers and the batch size increases. Specifically, the MAE and MSE converge at 175 neurons for hidden layer 1 and 100 neurons for hidden layer 2, as depicted in Figs. 7 and 8 for specific wear rate and coefficient of friction. All combinations of Mean Squared Error and Mean Absolute Error exhibited downward trends when the batch size was set to 64. Based on the information provided in Table 4 and Table 5, it is evident that the combination of ReLU activation function, and a neural network architecture with 175 neurons for layer 1 and 100 neurons for layer 2, along with a batch size of 64, resulted in the lowest Mean Squared Error and Mean Absolute Error. Thus, 175 neurons for hidden layer 1 and 100 neurons for hidden layer 2 are chosen to optimize the other hyperparameters with a batch size of 64.

### *3.3 Epoch and learning rate optimization*

The epoch number refers to the total number of iterations that the learning algorithm will perform on the training dataset. A crucial hyperparameter for fine-tuning the ANN model and achieving better model performance is the learning rate. Therefore, the optimum prediction ANN model can only be found by optimizing the learning rate and epochs (Sivaprasad *et al*. 2023) The Adam algorithm is employed as an optimizer to adjust the ANN model's attributes (Fei *et al*. 2020). The ANN model from the previous section is used to adjust the learning rates and epoch. It is evident from Figs. 9 and 10 that the MAE and MSE fall with increasing learning rate and epochs. Therefore, Lr = 0.01 is chosen for the MAE and MSE, respectively. The ReLu activation function with epoch 2000 and Lr = 0.01 resulted in the least MSE and MAE at the chosen learning rates for specific wear rate and coefficient of friction. The final optimized ANN model demonstrated the lowest error when using ReLU with MSE and MAE. Therefore, the final optimized model is selected to be ReLu with MSE using 175 hidden neurons for layer 1 and 100 hidden neurons for layer 2. The model is trained using a batch size of 64, a learning rate of 0.01, and for a total of 2000 epochs. Table 6 shows ReLU activation function values with MAE and MSE loss functions for different quantities of neurons in hidden layers 1 and 2.

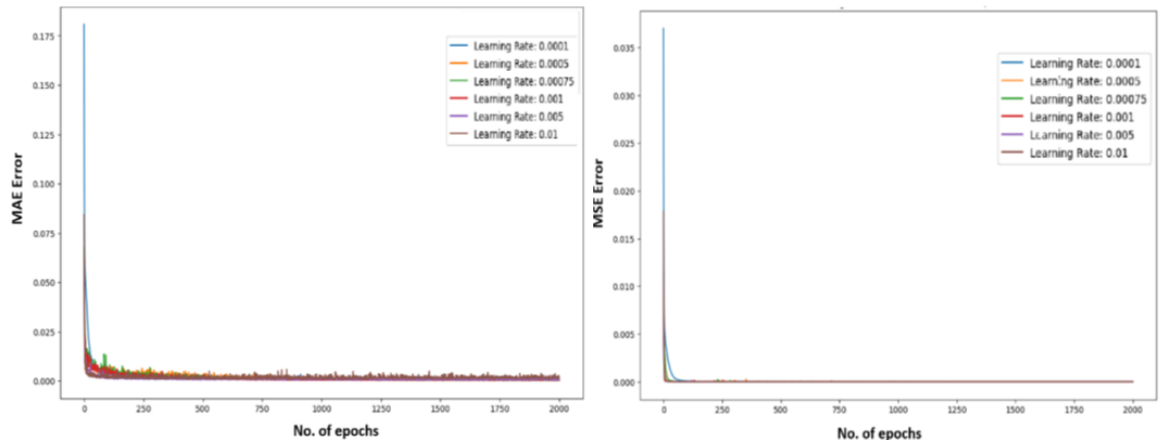


Fig. 10 Variation of a) MAE b) MSE for test data set for different learning rates and epochs for coefficient of friction

Table 6 Optimized training model based on training and testing

| Activation function | Cost function | No. of hidden neurons (Hidden layer 1) | No. of hidden neurons (Hidden layer 2) | Batch size | Learning rate | Epoch |
|---|---|---|---|---|---|---|
| ReLU | MAE<br>MSE | 175 | 100 | 64 | 0.01 | 2000 |

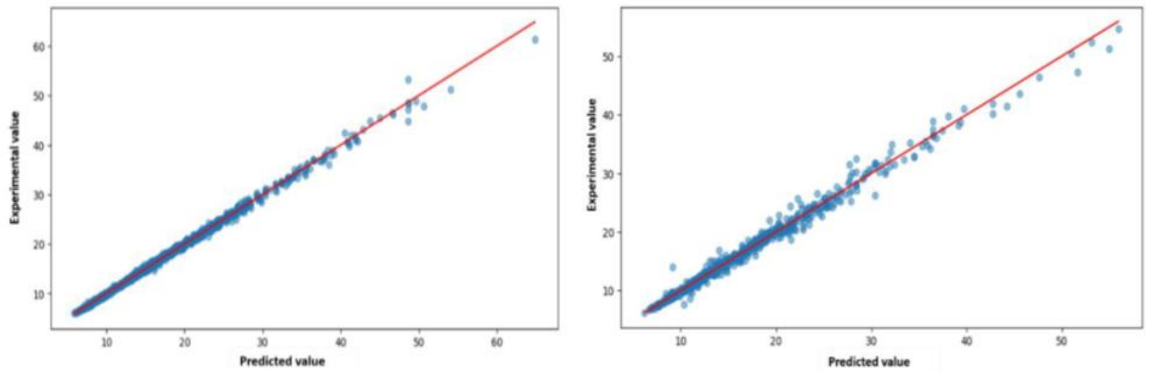


Fig. 11 Comparison between predicted and experimental responses of specific wear rate for a) training dataset b) Test dataset

### *3.4 Evaluation of Artificial Neural Network (ANN) model*

The ANN model is used to forecast the tribological features. It utilizes the ReLu activation function and the MSE and MAE loss functions for the hidden layers. The hidden layers consist of 175 neurons in layer 1 and 100 neurons in layer 2. The artificial neural network model is trained using a batch size of 64 and a learning rate (Lr) of 0.01. A dataset consisting of 1920 cases has been created using six input parameters: Al8090 matrix volume, Titanium diboride volume, Graphene volume, load, sliding speed, and sliding distance. The related output includes particular specific wear rate and coefficient of friction. Out of these cases, 70% of the dataset is utilized for

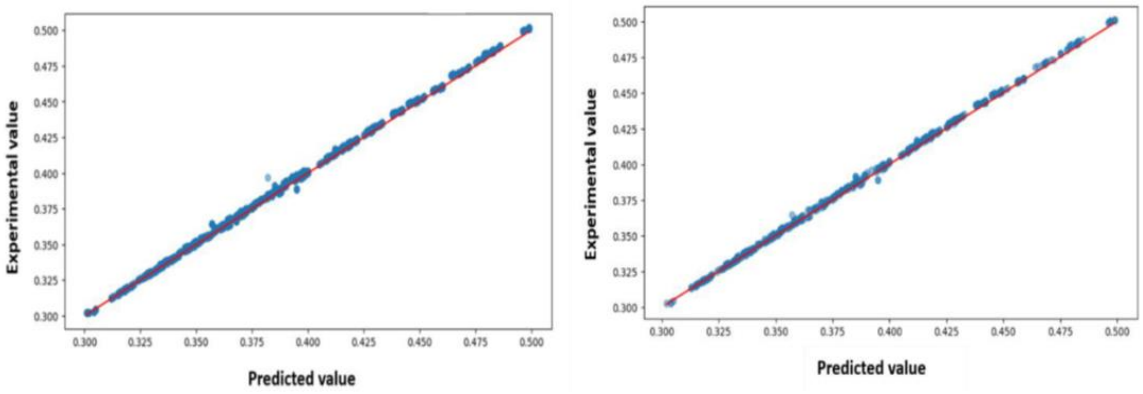


Fig. 12 Comparison between predicted and experimental responses of coefficient of friction for a) training dataset b) Test dataset

Table 7 Predicting the accuracy of an Artificial Neural Network (ANN) model

| Metric | Specific wear rate - Training | Specific wear rate - Testing | Coefficient of friction - Training | Coefficient of friction - Testing |
|---|---|---|---|---|
| MAPE (%) | 1.53 | 3.42 | 0.27 | 0.28 |
| $R^2$ | 0.99 | 0.99 | 0.99 | 0.99 |
| RMSE | 0.39 | 0.95 | 0.001 | 0.001 |

training the ANN model and for fine-tuning the hyperparameters. Ultimately, a test dataset comprising 30% of the data is employed to evaluate the precision of the Artificial Neural Network (ANN) model.

Figs. 11 and 12 displays the comparison between the specific wear rate and coefficient of friction predicted by the Artificial Neural Network (ANN) model and those obtained during wear testing. It has been established that the majority of data points in both the training and testing datasets are in close proximity to the line of best fit, as shown by the red line. This confirms that the prediction made by the established ANN model aligns closely with results obtained from wear test. The prediction accuracy of the ANN model for both datasets is shown in Table 7. The $R^2$ value for the test dataset is 0.99 which indicates a strong correlation with both specific wear rate and coefficient of friction. The MAPE values are 3.42% and 0.28% and RMSE are 0.95 and 0.001. This demonstrates that the well-established Artificial Neural Network (ANN) model possesses the capacity to acquire knowledge from novel data and exhibits strong concordance with the actual computed tribological characteristics. Therefore, the existing ANN model can be utilized as a predictive method for forecasting tribological characteristics. Using a predetermined collection of input parameters.

Fig. 13 shows variation of specific wear rate of Al8090/$TiB_2$/C composites. The wear rate of Al8090/10%$TiB_2$/2%C (11.56 x $10^{-5}$ $mm^3$/NM) was very low in compare to Al8090/8%$TiB_2$/2%C (12.21 x $10^{-5}$ $mm^3$/NM), Al8090/6%$TiB_2$/2%C (14.06 x $10^{-5}$ $mm^3$/NM), Al8090/4%$TiB_2$/2%C (15.41 x $10^{-5}$ $mm^3$/NM) and Al8090/2%$TiB_2$/2%C (17.06 x $10^{-5}$ $mm^3$/NM) composites due to addition of higher wt% of titanium diboride and graphene which results in higher hardness of composite. The wear characteristics, which include the friction coefficient and specific wear rate, are depicted in Fig. 13 as a function of the weight percentage of titanium diboride and graphene.

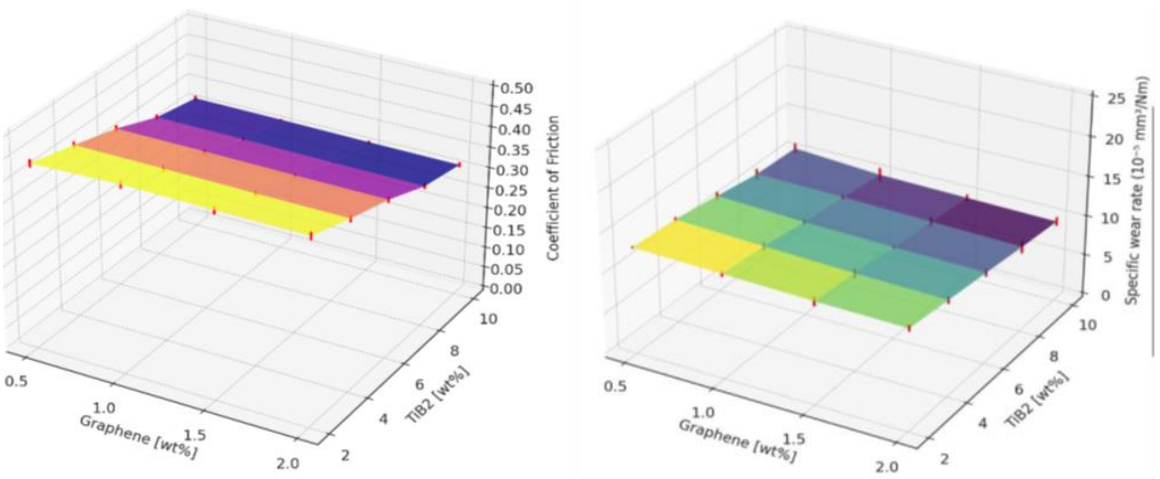


Fig. 13 Results of A) Coefficient of friction b) Specific wear rate with normal force 20 N and sliding speed 2 m/s for 30 min. measured data points with error bars are also shown

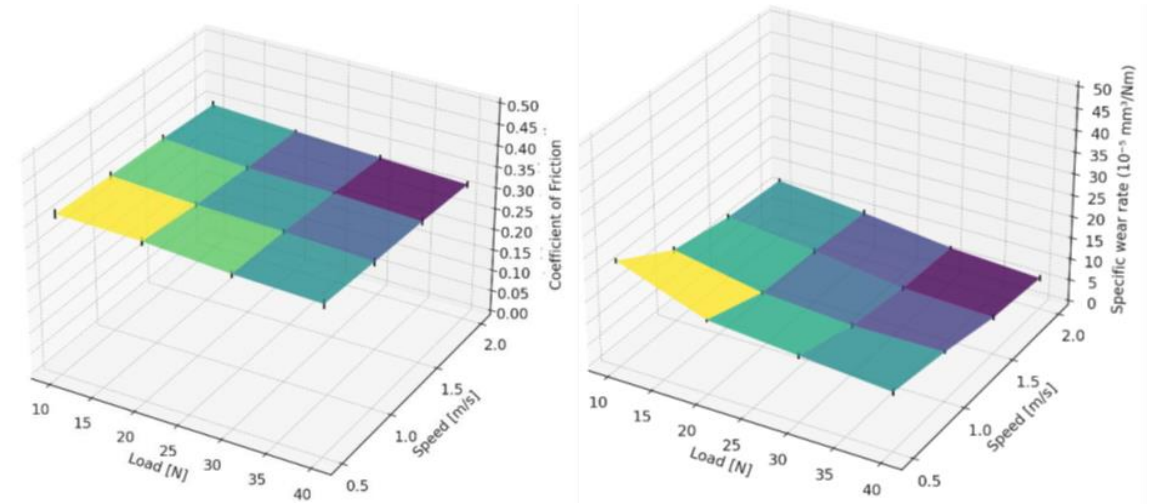


Fig. 14 Results of A) Coefficient of friction b) Specific wear rate as a function of normal force and sliding speed. [Matrix = 90%, graphene = 2%, and TiB2 powder = 8%]. Measured data points with error bars are also shown

These characteristics were determined under 20N and 2m/s for a duration of 30 mins. It has been noted that the wear resistance of the Al8090/$TiB_2$/C improves as a consequence of the incorporation of graphene which exhibit a higher thermal conductivity than the Al8090 matrix which leads to a reduction in the amount of heat that is generated in the sliding contact area (Zhang *et al*. 2024, Anuar *et al*. 2024). Additionally, it was discovered that the higher bonding strength of the transfer film that was created on the metallic counterface, results to the creation of a wear resistant Al8090/$TiB_2$/C composite (He *et al*. 2024, Babu *et al*. 2024). The data presents the specific wear rate and friction coefficient of the Al8090/$TiB_2$/C composite (with a matrix content of 90 wt%, graphene 2 wt%, and titanium powder 8 wt%) determined by testing conditions,

including sliding speed and normal force as shown in Fig. 14. The accuracy of these projected 3D planes is substantiated by the measurement results, which are accompanied by error bars.

## 4. Conclusions

The current study introduces a novel technique for efficiently predicting tribological parameters, such as specific wear rate and coefficient of friction, for Al8090 based hybrid composites using artificial neural networks. The framework takes as input the volume of Al8090 matrix, Titanium diboride, and Graphene, as well as the load, sliding speed, and sliding distance. The output of the framework is the specific wear rate and coefficient of friction.

• The wear resistance of Al8090/$TiB_2$/C composite increased with the addition of reinforcements such as Titanium diboride, and Graphene. Al8090/10%$TiB_2$/2%C has the highest wear resistance and least coefficient of friction in compare to Al8090 only.

• The optimized artificial neural network model comprises of input layer having 6 input parameters, 175 and 100 neurons for hidden layers and a output layer to calculate the specific wear rate and coefficient of friction.

• The optimized model employs Rectified Linear Unit (ReLU) as the activation function in the hidden layers. After computation, it was determined that using a batch size of 64 and a learning rate of 0.01 resulted in the lowest error when measuring squared error and mean absolute error as the cost function. These experiments were conducted across 2000 epochs.

• The mean absolute percentage error (MAPE) for the specific wear rate and coefficient of friction test cases was 3.42% and 0.28%, coefficient of determination ($R^2$) is 0.99 and 0.99, Root mean square error (RMSE) is 0.95 and 0.001 respectively. This study shown that the suggested framework, utilizing neural network technology, has the ability to decrease the time required for predicting the tribological characteristics of Al8090/$TiB_2$/C composites.

## Acknowledgement

The funding was received for conducting this study from AICTE.

## References

Afape, J.O., Willoughby, A.A., Sanyaolu, M.E., Obiyemi, O.O., Moloi, K., Jooda, J.O. and Dairo, O.F. (2024), "Improving millimetre-wave path loss estimation using automated hyperparameter-tuned stacking ensemble regression machine learning", *Results Eng*., **22**, 102289. https://doi.org/10.1016/j.rineng.2024.102289.

Akin, I. and Kaya, O. (2017), "Microstructures and properties of silicon carbide- and graphene nanoplatelet-reinforced titanium diboride composites", *J. Alloys Compd*., **729**, 949-959. https://doi.org/10.1016/j.jallcom.2017.09.244.

Anuar, N.F.B.W., Omar, M.Z., Salleh, M.S., Zamri, W.F.H.W. and Ali, A.M. (2024), "Effect of graphene addition on microstructure and wear behaviour of the A356-based composite fabricated by thixoforming process", *J. Mater. Res. Technol*., **30**, 4813-4831. https://doi.org/10.1016/j.jmrt.2024.04.192.

Azad, M.M. and Kim, H.S. (2024), "Hybrid deep convolutional networks for the autonomous damage diagnosis of laminated composite structures", *Compos. Struct*., **329**, 117792. https://doi.org/10.1016/j.compstruct.2023.117792.

Babaei, M., Atasoy, A., Hajirasouliha, I., Mollaei, S. and Jalilkhani, M. (2022), "Numerical solution of beam equation using neural networks and evolutionary optimization tools", *Adv Comput. Des.*, **7**, 1-17. https://doi.org/10.12989/acd.2022.7.1.001

Babu, R.R., Rajendran, C., Saiyathibrahim, A. and Velu, R. (2024), "Influence of B4C and ZrB2 reinforcements on microstructural, mechanical and wear behaviour of AA 2014 aluminium matrix hybrid composites", *Defence Technol.*, **2024**. https://doi.org/10.1016/j.dt.2024.05.009.

Cheung, H.L., Uvdal, P. and Mirkhalaf, M. (2024), "Augmentation of scarce data—A new approach for deep-learning modeling of composites", *Compos. Sci. Technol.*, **249**, 110491. https://doi.org/10.1016/j.compscitech.2024.110491.

Fei, Z., Wu, Z., Xiao, Y., Ma, J. and He, W. (2020), "A new short-arc fitting method with high precision using Adam optimization algorithm", *Optik*, **212**, 164788. https://doi.org/10.1016/j.ijleo.2020.164788.

González, A., Martín, J. and Llorca, J. (2004), "Effect of temperature on the fracture mechanisms of 8090 Al–Li alloy and 8090 Al–Li/SiC composite", *Scripta Materialia*, **51**, 1111-1115. https://doi.org/10.1016/j.scriptamat.2004.07.025.

Hasan, M.M., Rahman, M.M., Islam, M.S., Chan, W.H., Alginahi, Y.M., Kabir, M.N., Bakar, A. and Ramasamy, D. (2024), "Artificial neural network modeling for predicting thermal conductivity of EG/ Water-based CNC nanofluid for engine cooling using different activation functions", *Front. Heat Mass Transf.*, **22**, 537-556. https://doi.org/10.32604/fhmt.2024.047428.

He, W., Li, H., Han, X., Wang, X., Wang, G., Zhang, X. and Shcheretskyi, O. (2024), "High-temperature dry sliding friction and wear behavior of in-situ (Al3Zr+ZrB2)/AA6016 aluminum matrix composites", *Mater. Today Commun.*, **39**, 108951. https://doi.org/10.1016/j.mtcomm.2024.108951.

Jung, K.C. and Chang, S.H. (2021), "Advanced deep learning model-based impact characterization method for composite laminates", *Compos. Sci. Technol.*, **207**, 108713. https://doi.org/10.1016/j.compscitech.2021.108713.

Kazi, M.K., Eljack, F. and Mahdi (2020), "Predictive ANN models for varying filler content for cotton fiber/PVC composites based on experimental load displacement curves", *Compos. Struct.*, **254**, 112885. https://doi.org/10.1016/j.compstruct.2020.112885.

Kumar, J.L., Gurusamy, P., Gayathri, N. and Muthuraman, V. (2024), "Influence of graphene nanoplates and titanium diboride particulate on wear and interfacial bonding properties of sintered aluminium alloy composites", *Diamond Related Mater.*, **144**, 111035. https://doi.org/10.1016/j.diamond.2024.111035.

Lima, J.P.S., Evangelista Jr., F. and Soares, C.G. (2023), "Hyperparameter-optimized multi-fidelity deep neural network model associated with subset simulation for structural reliability analysis", *Reliabil. Eng. Syst. Safe.*, **239**, 109492. https://doi.org/10.1016/j.ress.2023.109492.

Lujan-Moreno, G.A., Howard, P.R., Rojas, O.G. and Montgomery, D.C. (2018), "Design of experiments and response surface methodology to tune machine learning hyperparameters, with a random forest case-study", *Exp. Syst. Appl.*, **109**, 195-205. https://doi.org/10.1016/j.eswa.2018.05.024.

Lynch, P., Muddle, B.C. and Pasang, T. (2001), "Ductile-to-brittle fracture transitions in 8090 Al–Li alloys", *Acta Materialia*, **49**, 2863-2874. https://doi.org/10.1016/S1359-6454(01)00217-8.

Manu, M., Aravind, J., Mohammed, S.B., Roy, K.E.R., Ali, M.M. and Shaik, U. (2024), "Optimization of tribological characteristics in cryo-treated plastic/graphene oxide modified CFRP via ANN-based predictive modeling for aerospace applications", *Compos. Sci. Technol.*, **250**, 110520. https://doi.org/10.1016/j.compscitech.2024.110520.

Protyai, M.I.H., Adib, F.M., Taher, T.I., Karim, M.R., Rashid, A.B. and Mahmud, F. (2024), "Performance evaluation of Kevlar fiber reinforced epoxy composite by depositing graphene/SiC/Al2O3 Nanoparticles", *Hybr. Adv.*, **6**, 100245. https://doi.org/10.1016/j.hybadv.2024.100245.

Provencher, B., Badran, A., Kroll, J. and Marsh, M. (2024), "Hyperparameter tuning for deep learning semantic image segmentation of micro computed tomography scanned fiber-reinforced composites", *Tomography Mater. Struct.*, **3**, 100032. https://doi.org/10.1016/j.tmater.2024.100032.

Santo, J., Pradhik, V., Kalakoti, S., Saravanan, P. and Penumakala, P.K. (2024), "Effect of composite processing technique on tribological properties of 3D printed PLA-graphene composites", *Tribol. Int.*, **2024**, 109895. https://doi.org/10.1016/j.triboint.2024.109895.

Singh, L.B., Jinu, G.R., Manoj, M. and Perumal, E. (2022), "Tribological behaviour of Al8090-SiC metal matrix composites with dissimilar B4C addition", *Silicon*, **14**, 8895-8908. https://doi.org/10.1007/s12633-021-01608-0.

Sivaprasad, H., Lekkala, M.R., Latheef, M., Seo, J., Yoo, K., Jin, C. and Kim, D.K. (2023), "Fatigue damage prediction of top tensioned riser subjected to vortex-induced vibrations using artificial neural networks", *Ocean Eng*., **268**, 113393. https://doi.org/10.1016/j.oceaneng.2022.113393.

Wang, W.C., Nguyen, N.M. and Cao, M.T. (2022), "Smart ensemble machine learner with hyperparameter-free for predicting bond capacity of FRP-to-concrete interface: Multi-national data", *Constr*. *Build*. *Mater*., **345**, 128158. https://doi.org/10.1016/j.conbuildmat.2022.128158.

Wang, B., Li, N., Bao, Q., Cheng, S., Feng, J., Li, M., Wang, N., Wang, Z., Jiang, B., Chen, L., Hong, H. and Jian, X. (2024), "Graphene at different scales to synergistically optimize the thermal and mechanical properties of CF/PPBESK composites", *Compos*. *Part B Eng*., **284**, 111692. https://doi.org/10.1016/j.compositesb.2024.111692.

Wang, Z., Zhao, C., Yang, Z., Wang, K., Dong, G. and Starostenkov, M.D. (2024), "Multi-scale collaborative prediction of optimal configuration for carbon fiber woven composites based on deep learning neural networks", *Compos*. *Struct*., **339**, 118165. https://doi.org/10.1016/j.compstruct.2024.118165.

Yu, X., Jiang, R., Gao, Y., Li, Y., Gong, W., Li, X. and Lü, W. (2024), "Microstructure and wear-resistant behaviors of Al2O3-TiO2 reinforced Ni-based composite coating plasma-sprayed on 6061 aluminum alloy", *Surf*. *Coatings Technol*., **487**, 131032. https://doi.org/10.1016/j.surfcoat.2024.131032.

Zhang, Y., Lv, Z., Cao, J., Tong, Y., Sun, M., Cui, C. and Wang, X. (2024), "Effect of SiC and TiC content on microstructure and wear behavior of Ni-based composite coating manufactured by laser cladding on Ti–6Al–4V", *Wear*, **15**, 205431. https://doi.org/10.1016/j.wear.2024.205431.

Zhou, S., Zhang, W., Liu, M., Ren, W., Zhou, Q., Wei, J. and Wu, P. (2023), "Strength-toughness combination in nickel matrix composites reinforced by hybrid graphene nanoplatelets-titanium diboride", *Carbon*, **201**, 1137-1148. https://doi.org/10.1016/j.carbon.2022.10.033.

*CC*